Engineering Structures 235 (2021) 112128

Contents lists available at ScienceDirect

Engineering Structures

journal homepage: www.elsevier.com/locate/engstruct

An analytical model describing the in-plane behaviour of timber diaphragms strengthened with plywood panels

Michele Mirra [a,*], Geert Ravenshorst [a], Peter de Vries [a], Jan-Willem van de Kuilen [a,b]

[a] Department of Engineering Structures, Biobased Structures and Materials Group, Delft University of Technology, Stevinweg 1, 2628 CN Delft, the Netherlands
[b] Wood Technology, Technical University of Munich, Winzererstrasse 45, 80797 Munich, Germany

ARTICLE INFO

Keywords:
Timber floors
Seismic rehabilitation
Analytical model
Plywood panels
Retrofitting

ABSTRACT

Timber diaphragms in existing buildings are often too flexible in their plane, and can thus potentially cause out-of-plane collapses of walls during earthquakes. A very efficient retrofitting method to increase their in-plane stiffness and energy dissipation is the overlay of plywood panels. However, the usual characterization of the floors by means of a general equivalent shear stiffness cannot account for their nonlinearity and dissipative properties. Therefore, in this work, an analytical model is formulated to describe the in-plane response of timber diaphragms strengthened with plywood panels screwed along their perimeter to the existing sheathing. The proposed formulation starts from the definition of the load-slip equation for a single screw connecting a plank and a plywood panel. The whole floor's response is then derived, with the prediction of both backbone curve and pinching cycles. From the comparison between the response of tested full-scale diaphragms and the analytically calculated one, it can be concluded that the proposed model accurately predicts the in-plane behaviour and dissipative properties of timber floors retrofitted with plywood panels.

1. Introduction

1.1. Background

Seismic rehabilitation of existing buildings is a key topic for many countries, because it allows to maintain and preserve their typical architectural heritage. A large part of the existing or historical building stock is characterized by the presence of timber diaphragms that are often not suitable to withstand horizontal loads without large deflections, causing in many cases damages and collapses of the walls. Hence, several strengthening techniques have been investigated in the recent years [1–15], in order to enhance the seismic properties of the existing diaphragms. Among these techniques, reversible ones are often preferred because of their lower impact on the original configuration of the structure, especially when the building to be retrofitted is monumental or protected [16].

In this framework, a plywood panels overlay proved to not only stiffen the diaphragms, but also increase their energy dissipation [11–15]. The effectiveness of this method triggered the investigation of its application to the building stock in the area around Groningen (NL), where human-induced earthquakes caused by gas extraction have started to take place. Local constructions are mainly unreinforced masonry structures with timber floors. These buildings are very vulnerable to seismic events, because they were not designed to withstand such actions, not present in that region until recently.

Therefore, to gain more insight into the in-plane behaviour of timber diaphragms with Dutch features, an experimental campaign and an analytical study were conducted (Fig. 1). The floors were firstly tested in their as-built configuration, and then retested after strengthening them with a plywood panels overlay [14]. With reference to the retrofitted diaphragms, five full-scale samples representing half of a floor were tested in a vertical configuration (Fig. 2): two specimens were tested parallel to the joists (*DFpar-1s*, *DFpar-2s*), two perpendicular to them (*DFper-3s*, *DFper-4s*), and one represented a roof pitch (*DRpar-5s*). For all diaphragms, the panels were fastened along their perimeter with screws to the as-built floor planks. Besides, the influence of other elements improving shear transfer, such as timber blocks or steel angles, was evaluated. Further details on this experimental campaign can be found in [14].

The full-scale tests showed a great improvement in strength, stiffness and energy dissipation of the diaphragms after retrofitting. Therefore, an analytical study was carried out to thoroughly describe their in-plane

* Corresponding author.
E-mail addresses: M.Mirra@tudelft.nl (M. Mirra), G.J.P.Ravenshorst@tudelft.nl (G. Ravenshorst), P.A.deVries@tudelft.nl (P. de Vries), J.W.G.vandeKuilen@tudelft.nl, vandekuilen@hfm.tum.de (J.-W. van de Kuilen).

https://doi.org/10.1016/j.engstruct.2021.112128
Received 16 November 2020; Received in revised form 9 February 2021; Accepted 22 February 2021
Available online 10 March 2021

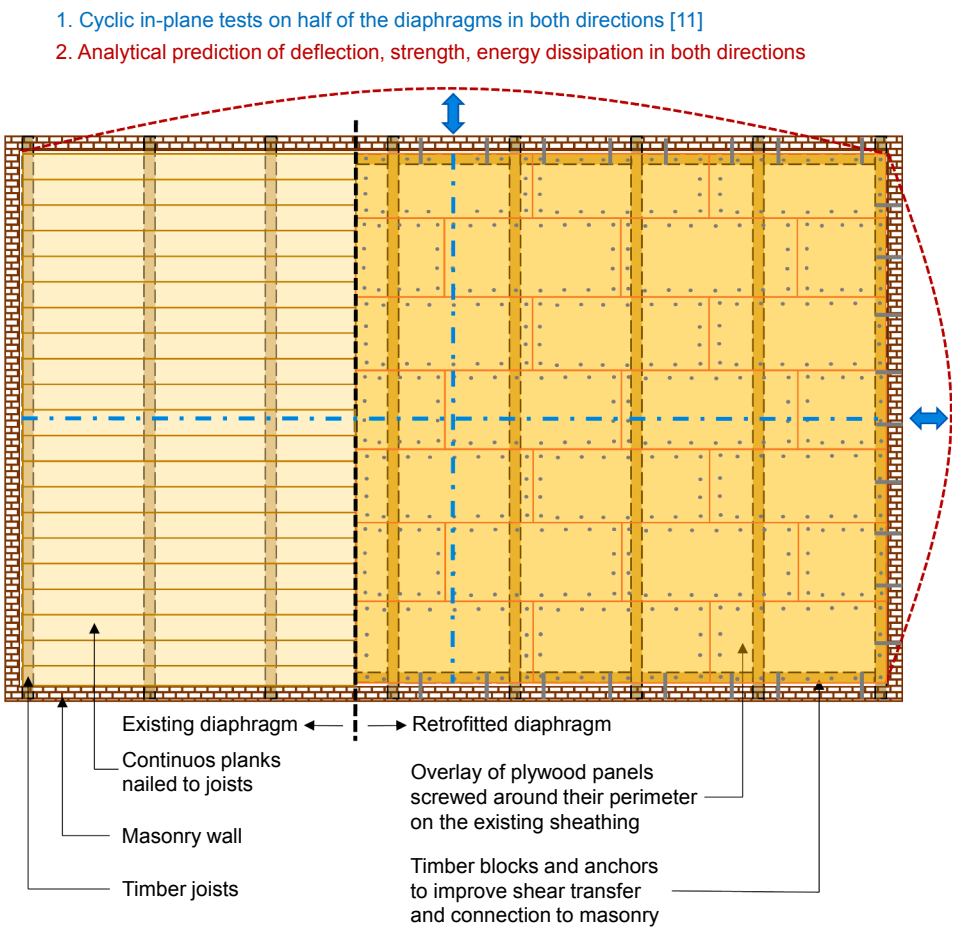

Fig. 1. Example of timber diaphragms retrofitted with a plywood panels overlay, and basic principles for the conducted tests [14], and for the formulation of the analytical model.

response. In this way, a general definition of equivalent shear stiffness, usually adopted to characterize the diaphragms, could be replaced by a more refined prediction of their strength, stiffness and energy dissipation, in both loading directions (Fig. 1). The formulated analytical model for refurbished floors is the subject of this article. The model enables a more detailed characterization of their in-plane behaviour, as well as a more precise design of the retrofitting intervention. This can be especially of help when considering the impact that the strengthening of the floors has on a whole building's response.

1.2. Research objective and approach

The objective of this work is to describe the in-plane response in terms of strength, stiffness, and energy dissipation of timber floors strengthened with plywood panels screwed along their perimeter to the existing sheathing. As starting point, the load-slip behaviour of the screws fastening planks and plywood panels is evaluated (Section 2): based on this, the global in-plane response of the diaphragm is then derived analytically (Section 3). Although the model was formulated to predict the response of floors with Dutch features, its definition is general and can be applied to other contexts as well, provided that the proposed retrofitting method is used, and an efficient shear transfer is ensured on the diaphragms sides, and to the walls (e.g. with timber blocks, steel angles, additional fasteners, etc.). The behaviour of the diaphragms is analysed when loading them both parallel and perpendicular to the joists, according to the principles of Fig. 1.

In order to generalize the formulated model, the methodology to derive the expression defining the load-slip behaviour of screws is presented in two cases:

1. Derivation from performed tests on plank-plywood panel connections;
2. Derivation through equations from current standards or literature.

The main assumptions at the basis of the proposed model are as follows:

- The shear load between panels can be transferred by the planks;
- Contact between plywood panels is taken into account as an increase in stiffness, according to the findings of [15];
- The rows of screws that are parallel to the load oppose to the panels sliding, while the ones that are perpendicular to the load have to withstand the panels rotation.

The derived formulation was then validated by comparing the response predicted with the analytical model to the one of tested diaphragms (Section 4). Furthermore, an example of implementation in finite element software is presented (Section 5).

2. Behaviour of the fasteners

2.1. Introduction

Since the proposed model aims to describe, starting from the single fasteners, the global in-plane behaviour of floors strengthened with plywood panels, the properties of these connectors have to be accurately defined.

Before arranging the experimental campaign on full-scale strengthened floors described in [14], tests were performed on fourteen small-

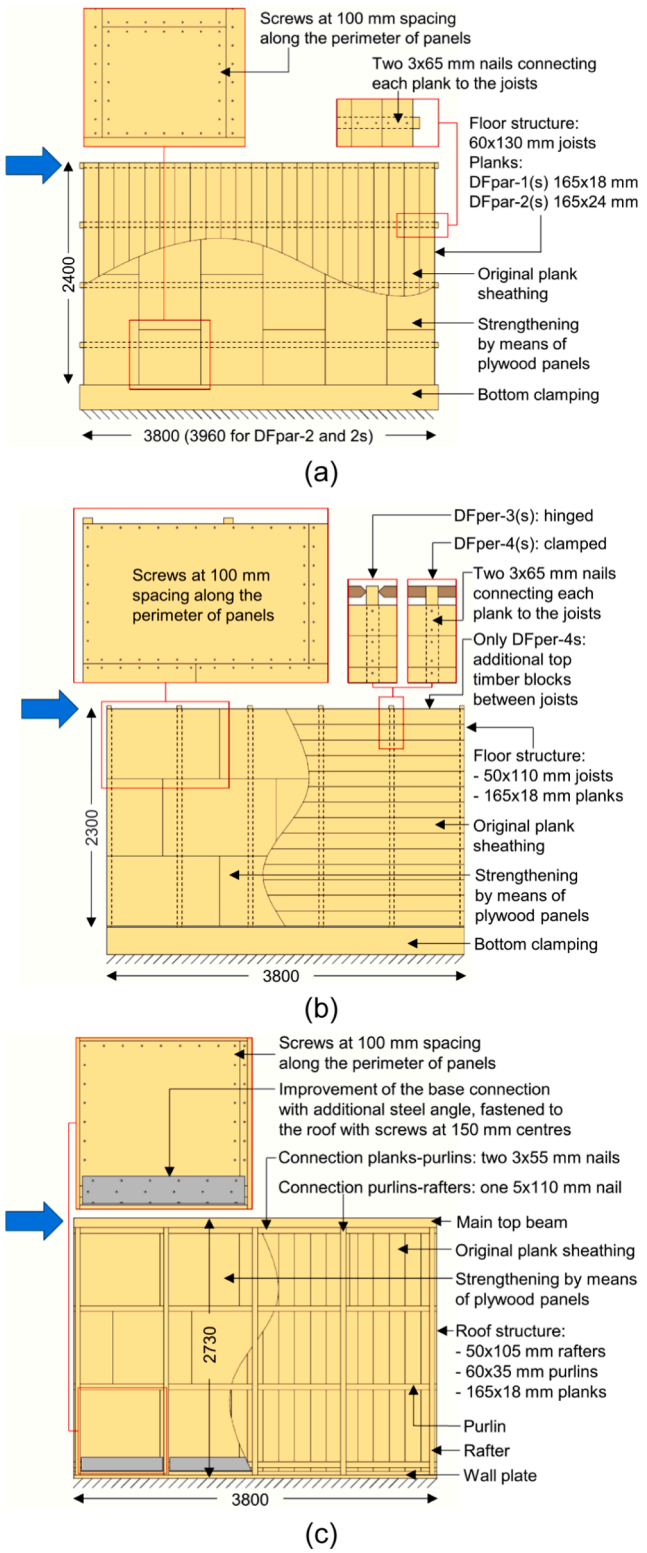

Fig. 2. Characteristics of the full-scale tested samples [14]: specimens tested parallel to joists (a), perpendicular to them (b) and roof pitch (c).

size replicates to assess the properties of the fasteners connecting the plywood panels to the planks. These specimens consisted of a portion of plank, to which part of a plywood panel was fastened by means of two screws, as shown in Fig. 3. The panel's main direction was arranged parallel to the plank's one, as it was done for the full-scale tests on floors. The adopted material was the same used for the construction of the whole diaphragms, therefore it represented an accurate replication of existing floors [14]. Both plywood panels and planks were made of spruce (*Picea Abies*), and had a thickness of 18 mm, while the screws had a diameter of 4.5 mm and a length of 40 mm.

Quasi-static reversed-cyclic shear tests were performed according to ISO 16670 [17]: seven replicates were tested parallel to the main direction of the plank, and the other seven orthogonal to it (Fig. 3a). Even if the obtained load-slip curves were similar between the two loading directions, in the graphs of section 2.2 they will be shown separately.

However, some of the full-scale strengthened floors did not present the same characteristics as the small-size replicates: sample *DFpar-2s* featured 24 mm planks, and in specimens *DFpar-2s*, *DFper-3s*, *DFper-4s* screws with a 5 mm diameter were used [14]; these variations are summarized in Table 1.

Thus, to predict the behaviour of all the diaphragms and to account for these variations, the derivation of the equation for the fasteners response was generalized: in this way, if tests are available, the expression can be derived following the same procedure described in Section 2.2; otherwise, the direct estimation of the load-slip behaviour remains still possible with the knowledge of basic material properties of timber and fasteners (Section 2.3).

2.2. Determination of the load–displacement relation of the fasteners from experimental tests

The determination of the load-slip curve for the screws is of fundamental importance for the description of the overall behaviour of the diaphragms: starting from an appropriate representation of the nonlinear behaviour of the fasteners, it is then possible to extend it to the whole system.

Therefore, firstly the backbone curves were constructed from the hysteretic cycles, following the procedure of ISO 16670 [17]. Secondly, to derive the adopted load-slip relation from the experimental tests, the curves corresponding to the third stabilized envelope were considered; the procedure was carried out separately for each loading direction. The negative backbones were included in the positive side of the graph: in total, 14 backbone curves were thus available for each loading direction. As a consequence, a possible asymmetric behaviour was not taken into account; yet, this assumption still allows to accurately capture the whole response of the diaphragms, as shown in Section 4.

It was chosen to model the load-slip response by means of a linear and a parabolic branch, representing the initial stiffness and the global behaviour, respectively. This procedure was followed for screws tested both parallel and orthogonally to the main direction of the planks, as shown in Fig. 4. The threshold for the choice of the experimental points representing the initial stiffness was fixed at a displacement of approximately 1 mm.

After determining these two branches (initial stiffness and global backbone), for a better representation, a continuous curve was created with an extension of Foschi's load-slip model for nails [18]. This consisted of an exponential curve linking together two straight lines, representing the initial and the post-yielding stiffness. The same principle was, thus, followed for the construction of the curve linking the initial stiffness line and the parabola representing the global response. By adopting this model, it is possible to take into account both post-yielding and softening behaviour of the fasteners. The equation of the curve is defined as:

$$F_s = \left(F_0 + a d_s + b d_s^2\right)\left[1 - e^{-\frac{K_0}{F_0} d_s}\right] \geq 0; \text{ with } a > 0,\ b < 0 \tag{1}$$

In Eq. (1), F_s and d_s are the force and displacement of the screw, respectively; F_0, a and b are the coefficients of the parabola representing the global behaviour, while K_0 is the slope of the line representing the initial stiffness. This curve (Fig. 5) fits the experimental points with $R^2 =$

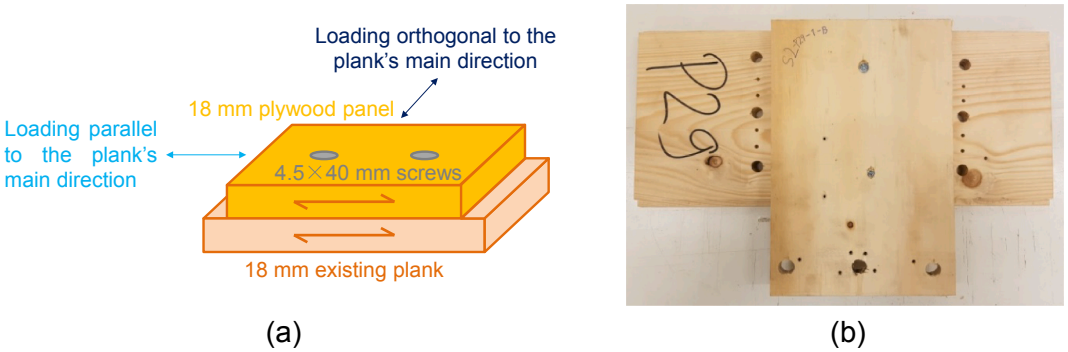

Fig. 3. Samples prepared for the tests on screws fastening the plywood panels to the existing sheathing: schematic description (a) and example of specimen (b).

Table 1
Variations in the characteristics of the full-scale tested diaphragms with respect to the small-size tests on screws fastening plywood panel and plank.

Full-scale sample	Variations with respect to small-size plank-plywood tests
DFpar-1s	None
DFpar-2s	Planks (24 mm), Screws ($d = 5$ mm)
DFper-3s	Screws ($d = 5$ mm)
DFper-4s	Screws ($d = 5$ mm)
DRpar-5s	None

0.83 when the panel is loaded parallel to the plank, and with $R^2 = 0.95$ if the force is applied perpendicular to it. As a failure criterion for the softening phase, the ultimate displacement can be considered as the one at which the maximum load has decreased by 20% after the peak, in agreement with the provisions of ISO 16670 [17] and EN 12512 [19].

As it is usually observed when analysing tests on timber joints, a scatter is present in the data points and the backbones: however, since a large number of screws is used in the whole floor, the global behaviour will tend to the average trend.

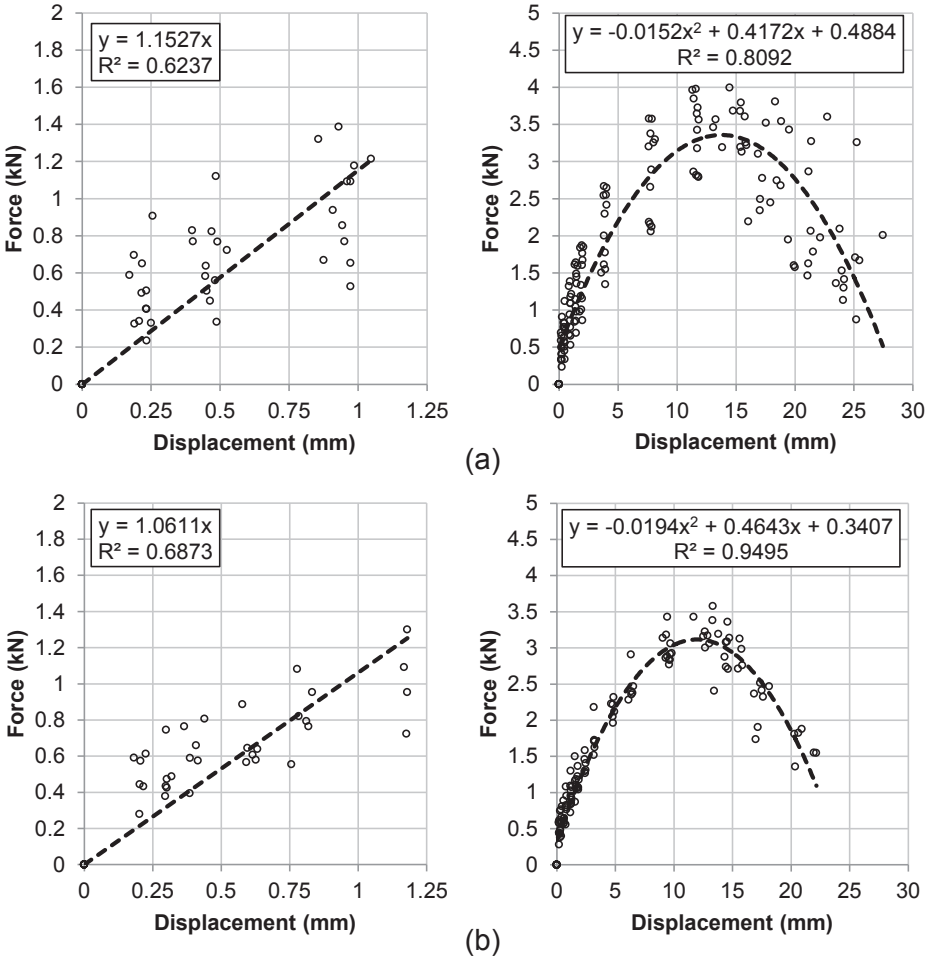

Fig. 4. Determination from experimental tests of the branches representing the initial stiffness and the global response of the screws when loading the plywood panel parallel to the plank (a) and perpendicular to it (b). Experimental data points correspond to each cycle's amplitude on the various backbones.

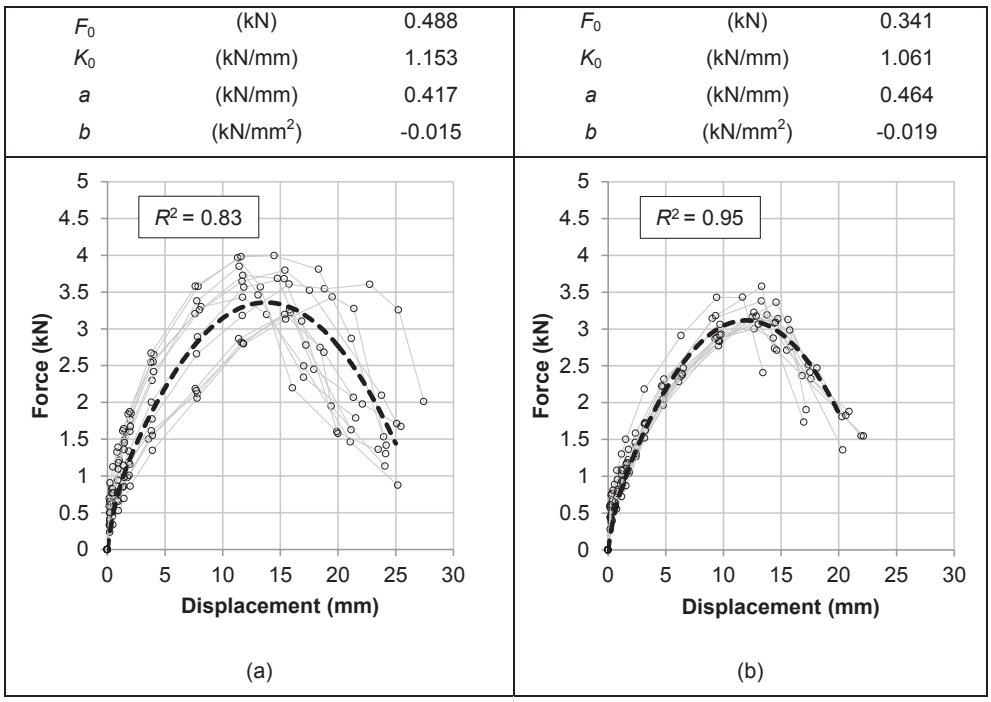

Fig. 5. Proposed load-slip curve (dashed) in comparison to the experimental data points and backbones for the direction parallel to planks (a) and perpendicular to them (b). The main parameters of the curve equation are also reported.

Table 2
Comparison among the values of initial stiffness K_0 for a single screw obtained experimentally and calculated according to equations from standards or literature.

Equation for K_0	Source	Value (kN/mm)
$50d^{1.7}$	Dubas et al. [20]	0.64
$\rho^{1.5}d^{0.8}/30$	Eurocode 5 [21]	1.08
$\rho^{1.5}d^{0.8}/25$	DIN 1052 [22]	1.30
–	Value from tests, // to plank	0.58
–	Value from tests, ⊥ to plank	0.53

2.3. Analytical derivation of the load–displacement relation of the fasteners

When tests are not available for determining the parameters K_0, F_0, a and b, an estimation of them with equations present in standards or literature is proposed as follows:

- K_0 can be determined with the expression provided in [20] for non-predrilled nails, using the nominal diameter d of the screw:

$$K_0 = 50d^{1.7} \tag{2}$$

Eq. (2) was chosen for its simplicity and very good agreement with the results obtained from the presented tests. Instead, relations provided by EN 1995 [21] and DIN 1052 [22] tended to overestimate K_0. Table 2 reports a comparison between the experimental values and the ones calculated adopting the aforementioned equations.

- F_0 can be predicted starting from the knowledge of the maximum force F_{max} determined according to EN 1995 [21] and Johansen's theory [24] for timber-to-timber joints, and with a screw sufficiently slender to develop two plastic hinges (this was also the failure mode observed in the tests):

$$F_{max} = \sqrt{\frac{2\beta}{1+\beta}}\sqrt{2Mf_{h,1}d} + \frac{F_{ax}}{4} \tag{3}$$

In the former equation, the usual factor 1.15 of the design expression was neglected, because the average material characteristics were used. The other parameters have the same meaning as in EN 1995, thus M is the plastic bending moment of the screw, $f_{h,1}$ is the embedment strength of the first joint's member, β is the ratio between the embedment strengths of the second and of the first member, d the nominal diameter of the screw, and F_{ax} the axial force developed because of the rope effect. The plastic bending moment is calculated with the screw's shank or inner diameter d_1, while for the embedment strength evaluation the

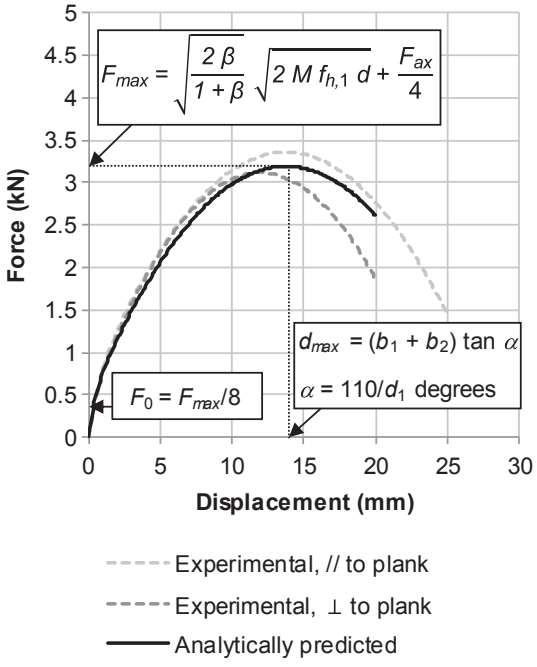

Fig. 6. Comparison between the analytically derived curve and the two ones obtained from the experimental data.

Table 3
Average measured material properties of the tested plank-plywood panel joints used for the derivation of the analytical curve.

Property	Average value
Density of plank ρ_1 (kg/m^3)	444
Density of plywood panel ρ_2 (kg/m^3)	469
Nominal screw diameter d (mm)	4.5
Screw's shank diameter d_1 (mm)	3.1
Tensile strength of screws f_u (MPa)	1000
Withdrawal resistance parameter f_{ax} (MPa)	17

Table 4
Calculated parameters based on diaphragms configurations (see Table 1). The variation in results compared to samples *DFpar-1s* and *DRpar-5s*, having the same properties as the reference tests on plank-plywood panel joints, is noticeable.

Property	Calculated value				
	DFpar-1s	*DFpar-2s*	*DFper-3s*	*DFper-4s*	*DRpar-5s*
Distance plastic hinge-plank's edge b_1 (mm)	11.3	13.7	13.7	13.7	11.3
Distance plastic hinge-panel's edge b_2 (mm)	7.9	9.6	9.6	9.6	7.9
Estimated bending angle (°)	35.5	29.7	29.7	29.7	35.5
Shear strength for 2 screws F_{max} (kN)	3.2	4.0	3.9	3.9	3.2
Estimated slip at peak force d_{max} (mm)	13.7	13.3	13.3	13.3	13.7

nominal one is adopted. Then, F_0 can be estimated as $F_{max}/8$.

- To determine the parameters a and b, it is necessary to identify three points crossed by the parabola. The last quantity to be estimated is, then, the slip d_{max} of the screw at F_{max}. To this end, firstly the expression of EN 409 [23] can be used for determining the angle α at which the screws bending moment is evaluated, and adopting for its calculation the shank or inner diameter d_1 of the screw (Eq. (4)). Secondly, the distance $(b_1 + b_2)$ between the two plastic hinges according to Johansen's theory [24] is determined (Eq. (5)). By combining these two quantities, the slip d_{max} can be estimated (Eq. (6)). Thus:

$$\alpha = \frac{110}{d_1}(\text{degrees}) \tag{4}$$

$$b_1 = \sqrt{\frac{2\beta}{1+\beta}}\sqrt{\frac{2M}{f_{h,1}d}} \text{ and } b_2 = \frac{b_1}{\beta} \tag{5}$$

$$d_{max} = (b_1 + b_2)\ \tan\ \alpha \tag{6}$$

After calculating the slip at F_{max}, the parabola is univocally determined by the three points $(0, F_0)$, (d_{max}, F_{max}), and $(2d_{max}, F_0)$. The two coefficients are then $a = 2(F_{max} - F_0)/d_{max}$ and $b = -(F_{max} - F_0)/(d_{max})^2$.

The aforementioned procedure led to obtain an estimated load-slip behaviour very close to the experimental ones: the comparison is shown in Fig. 6, together with a summary of the estimated parameters. The properties of the tested plank-plywood panel samples, used for the derivation of the load-slip analytical curve, are reported in Table 3. With this prediction, it was also possible to account for the different diaphragms configurations (Table 1), for which specific companion tests on plank-plywood panel joints were not performed. The results from these calculations are reported in Table 4: as can be noticed, the increase in screws diameter has a greater influence on the peak force than the presence of thicker planks (sample *DFpar-2s*).

Therefore, by adopting this procedure, it is possible to generalize the proposed expression also when tests are not available or material properties cannot be measured. It is sufficient to know, for instance, the properties of screws according to the producers, and the strength classes of planks and plywood.

3. Prediction of the global behaviour of the diaphragms

3.1. Principle of the developed procedure for both diaphragms loading directions

The proposed analytical model was developed by taking into account the stiffening intervention adopted for the experimental tests presented in [14]. In the following, the direction orthogonal to the in-plane load is identified as *vertical*, the one parallel to it as *horizontal*. The retrofitting took place by screwing plywood panels along their perimeter to the sheathing of the as-built existing floor, without having to consider the position of the underlying joists. This type of refurbishment is particularly advantageous, because the screws are placed in such a way that it is possible to identify their specific contribution to the overall resisting mechanism.

This aspect is more clearly depicted in Fig. 7a: when the strengthened floor is subjected to a horizontal load and the panels are vertically arranged, the force is subdivided among the columns of panels, and the screws are opposing to it with their stiffness. Each column of panels is subjected to rotation and sliding: the rocking behaviour is taken into account by considering the vertical screws, while the (very limited) slip is evaluated through the horizontal screws (Section 3.2). More precisely, due to the alternate configuration of the panels, the vertical number of screws is always fixed, while the horizontal one is considered as an average of two columns, as shown again in Fig. 7a.

When the pattern of the panels is composed of horizontal rows, a similar procedure can be followed, remembering that now the number of horizontal screws remains always the same, and a calculation has to be performed for the average number of vertical ones: this aspect is shown in Fig. 7b. In this case, consider for the same floor a vertical column composed of two whole panels and two halves of them, and another column in which the opposite situation is present (four halves and only one whole panel): as can be observed, the total number of horizontal screws remains the same independently from the considered column. This statement is valid also for the vertical screws, because when they are positioned at half of the width of the column, their number is doubled and their lever arm is half of the one of the vertical screws at the edges of the column. Therefore, the number of the central screws gives the same contribution as the one of the screws on the edges. Then, independently from the chosen way to consider a column, always the same number of screws is calculated. It is only important to count the number of columns needed to cover the whole floor coherently with the assumed configuration for the determination of one column (in this example *whole panel – two halves – whole panel* or *two halves – whole panel – two halves*).

3.2. Calculation of the in-plane deflection

When knowing the load-slip behaviour of screws (Section 2), for a certain displacement d_s of the fastener, a value F_s of force corresponds. Starting from these two parameters, it is possible to calculate the global deflection of the diaphragm according to the principle shown in Fig. 8, for vertically arranged panels.

The total horizontal load induces a rotation ϑ of each column of plywood panels, given by:

$$\vartheta = \frac{d_{s,v}}{w_c - e} \tag{7}$$

where $d_{s,v}$ is the displacement of one vertical screw, w_c is the width of the panels column, and e is the distance of the solicited vertical screws from the edge. The rotation point is considered to be at each panel corner because of the way of deflecting of a whole diaphragm, with contact

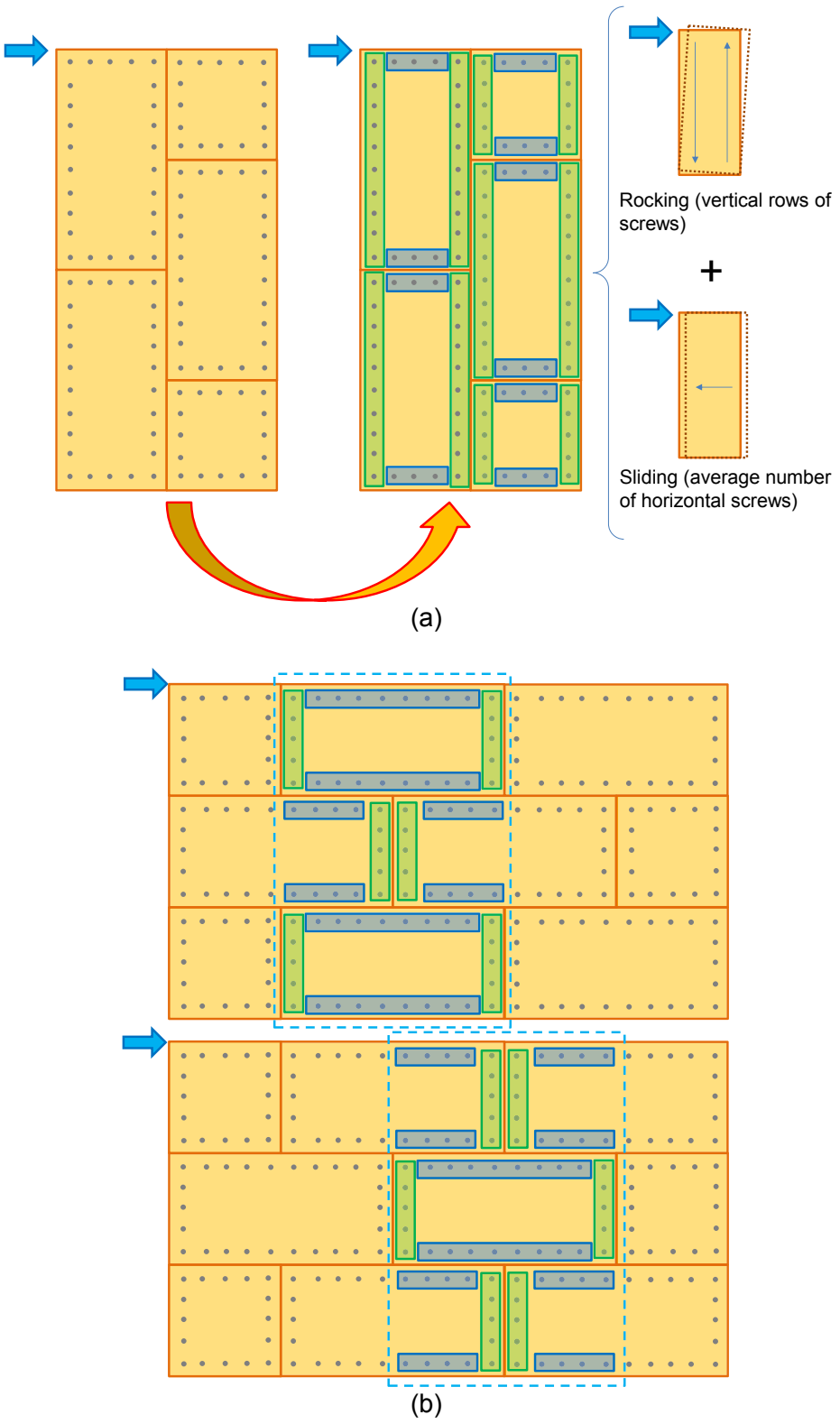

Fig. 7. (a) Principle of the analytical model formulated for the seismic design of the proposed strengthening technique, when the panels are arranged vertically; (b) individuation of the horizontal and vertical screws columns when the panels are arranged horizontally.

among panels (Fig. 8), as was observed during the tests as well [14]. This interlocking effect is then taken into account as an increment in horizontal load, as will be later shown. Should the panels be able to rotate more freely, for instance if a gap among them is left on purpose, the lever arm to be adopted would be $w_c - 2e$.

The horizontal displacement d_c reached on top of the column of panels (corresponding to the middle of the floor) is, thus:

$$d_c = \vartheta \cdot l_c \tag{8}$$

where l_c is the length of the panels column covering half of the

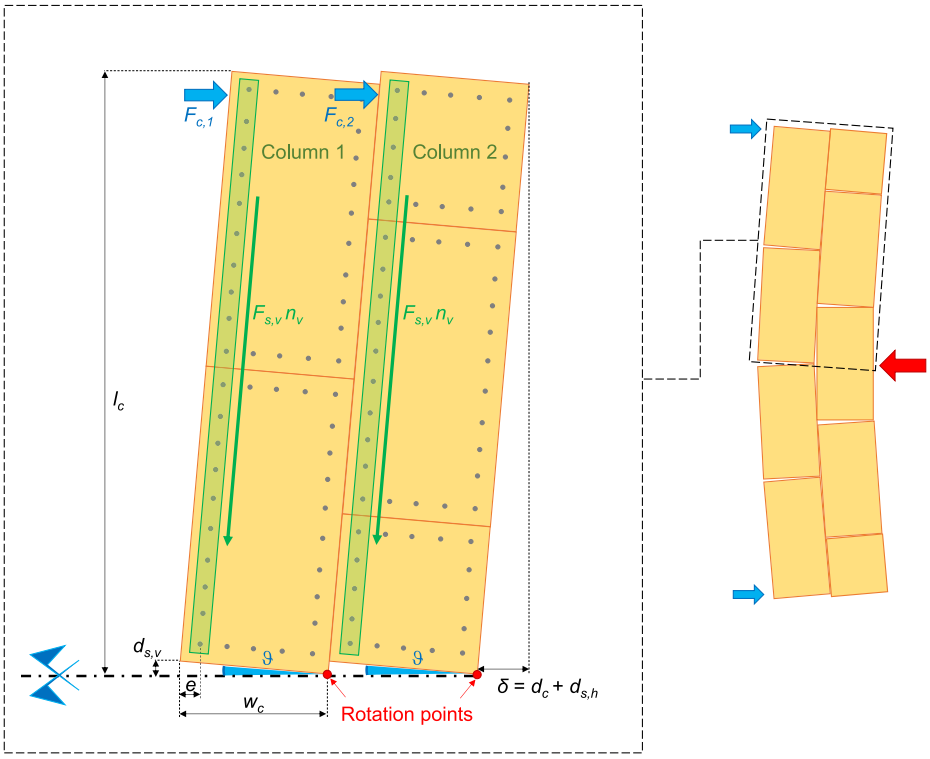

Fig. 8. Principle for the calculation of the global deflection of the floor from each panels column of panels.

diaphragm. Besides the displacement, also the horizontal load can be calculated by applying equilibrium, and starting from the force $F_{s,v}$ on a single vertical screw:

$$F_c = \frac{F_{s,v} \cdot n_v \cdot (w_c - e)}{l_c} \tag{9}$$

where n_v is the number of solicited vertical screws in a column and F_c the horizontal force activated in one column. Again, with panels able to rotate freely, the lever arm to be adopted is $w_c - 2e$.

After this step, by knowing the number of columns n_c, the total horizontal load F is calculated as:

$$F = n_c \cdot F_c \tag{10}$$

This force is referred to half of the diaphragm, and it therefore represents the shear that is transferred to the walls, while the resistance of the floor is given by $2F$. Furthermore, to account for panels interlocking due to the deflection of the diaphragm (Fig. 8), results from sensitivity analyses on several diaphragms configurations reported in [15] were considered. With a load parallel to the panels (e.g. as in Fig. 7b), a negligible interlocking effect was noticed. Instead, with the alternate disposition of Fig. 8 and a load orthogonal to the panels, a drift-dependent not negligible increment in stiffness was observed. From the results of [15], the following simplified expression was formulated to account for a drift-dependent force increment ΔF due to panels interlocking, to be used when the load is orthogonal to the panels and they have an alternate disposition (thus, only for samples *DFpar-1 s* and *DFpar-2 s*, in this case):

$$\Delta F = 1.05 + 10\frac{d_c}{l_c} \tag{11}$$

Thus, if panels interlocking is present:

$$F = \Delta F \cdot n_c \cdot F_c \tag{12}$$

Now, the slip of the column can be determined by considering the horizontal screws; the load $F_{s,h}$ on each one of them is given by:

Table 5
Values of the parameters used to predict the global floor's in-plane response according to the properties of tested samples.

Parameter		*DFpar-1s*	*DFpar-2s*	*DFper-3s*	*DFper-4s*	*DRpar-5s*
w_c	(mm)	670	670	1200	1200	825
e	(mm)	50	50	50	50	50
l_r	(mm)	2400	2400	2300	2300	2730
n_v		23	24	23	23	20
n_c		6	6	3	3	4.5
n_h		25	25	60	60	36

$$F_{s,h} = \frac{F}{n_c n_h} \tag{13}$$

where n_h is the total (or average, if the case) number of horizontal screws in a column of panels. From this value of $F_{s,h}$, the corresponding displacement $d_{s,h}$ is known, and consequently also the panels slip. Compared to the displacement due to rocking, this sliding is very limited (up to 1.8% of d_c for the analysed diaphragms). The total deflection of the floor is equal to:

$$\delta = d_c + d_{s,h} \tag{14}$$

The values of the aforementioned parameters for each tested diaphragm are reported in Table 5, and this procedure was followed for the determination of the in-plane deformation of the floor.

The results of this calculation are coherent with the static scheme that was adopted in the full-scale experimental tests [14]. However, in practice the load is not punctually applied in the middle of the floor, but distributed: to account for this, it is necessary to consider the pertaining static scheme. As an example, if a diaphragm with dimensions $B \times L \times t$ and shear modulus G can be regarded as a simply supported beam, then a distributed in-plane load $q = F/L$ would cause a deflection $\delta_q = q \cdot L^2/(8 \cdot G \cdot B \cdot t) = F \cdot L/(8 \cdot G \cdot B \cdot t)$ instead of $\delta_F = F \cdot L/(4 \cdot G \cdot B \cdot t)$. This means that the floor's force–displacement relation calculated with the analytical model has to be modified by considering a halved deflection.

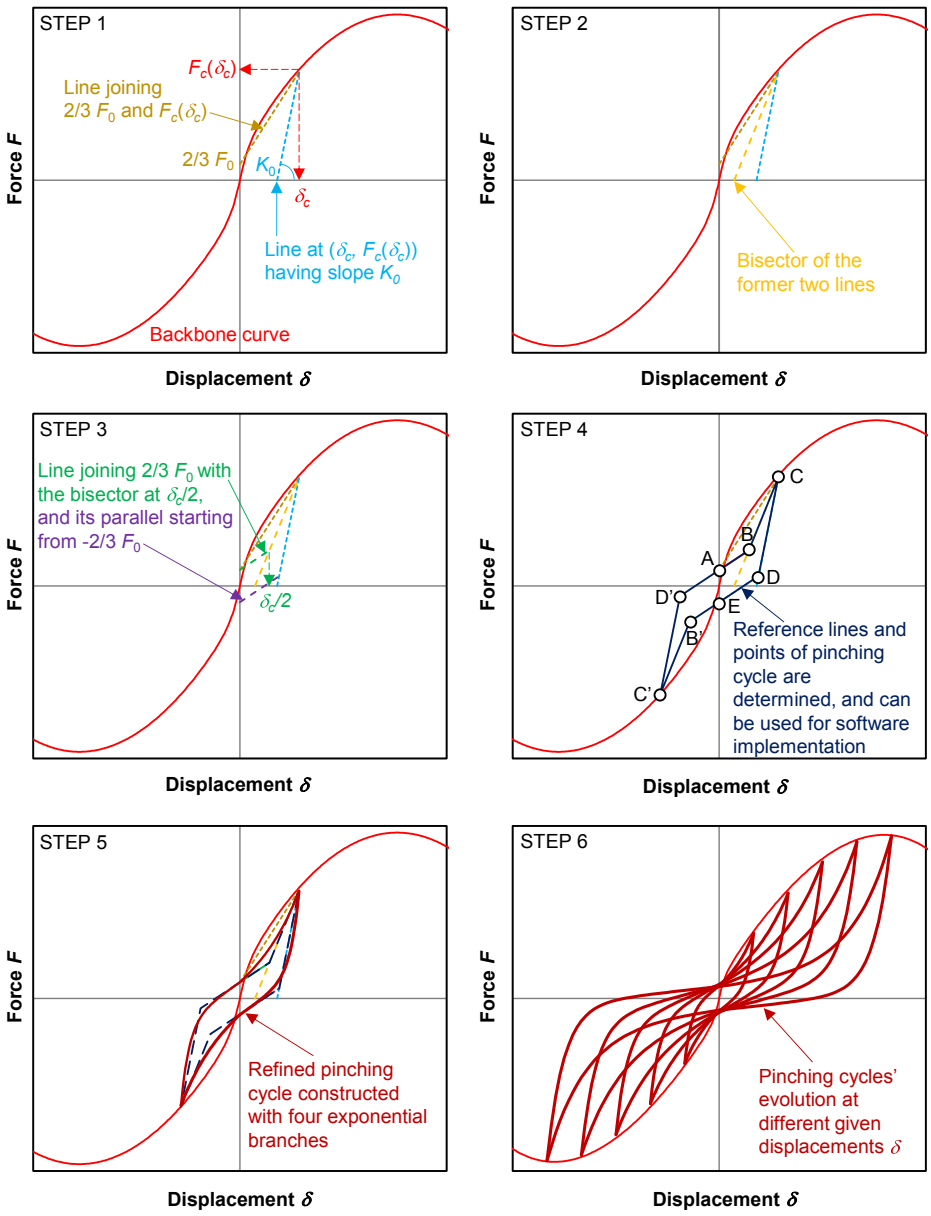

Fig. 9. Procedure for the determination of the pinching cycles from the analytical backbone curve.

3.3. *Pinching cycles prediction from backbone curve in full-scale tests*

The procedure shown in Section 3.2 allows to determine, starting from the proposed analytical curve representing the load-slip response of screws (Section 2), the global force–displacement backbone of the diaphragms. In addition to that, an estimation of the internal pinching cycles is of importance for both assessing the dissipative properties of the floors, and implementing their full response in a numerical model.

Therefore, a method was developed to estimate the pinching cycles from the proposed curve. The procedure starts from identifying a succession of linear branches, similarly to the *Pinching4* material [25] implemented in the software *OpenSees* [26]. The reference points are defined according to the procedure shown in Fig. 9, on the basis of geometrical considerations.

The pinching behaviour implies the presence of a residual force at zero displacement: this load is in general approximately corresponding to the force that leads to the very first yielding of the tested sample. In the analytical curve equation, F_0 is the intercept on the *y*-axis (force) of the parabola representing the global response of the specimens: in order to capture the very first yielding on the analytical curve, the intercept on the *y*-axis assumed for the pinching cycle is $2/3F_0$, a value around which the curve's initial slope starts to change.

After having considered this first intercept, the pinching cycle can be determined for a certain amplitude identified by a point (δ_c, $F_c(\delta_c)$) on the curve. As a first step, two lines are determined: one joining the points (0, $2/3F_0$) and (δ_c, $F_c(\delta_c)$), and one crossing the point (δ_c, $F_c(\delta_c)$) with slope K_0 (Fig. 9, step 1). Then, the bisector of these two lines is found (step 2). In step 3, the remaining part of the cycle is defined: firstly, the line joining (0, $2/3F_0$) and the point on the bisector having *x*-coordinate equal to $\delta_c/2$ is determined; secondly, a line parallel to the former one intersects the branch having slope K_0, starting from the point (0, $-2/3F_0$).

In step 4, the whole multilinear cycle is thus determined by the following points, identified by the previous branches and reported clockwise (Fig. 9):

A. (0, $2/3F_0$);

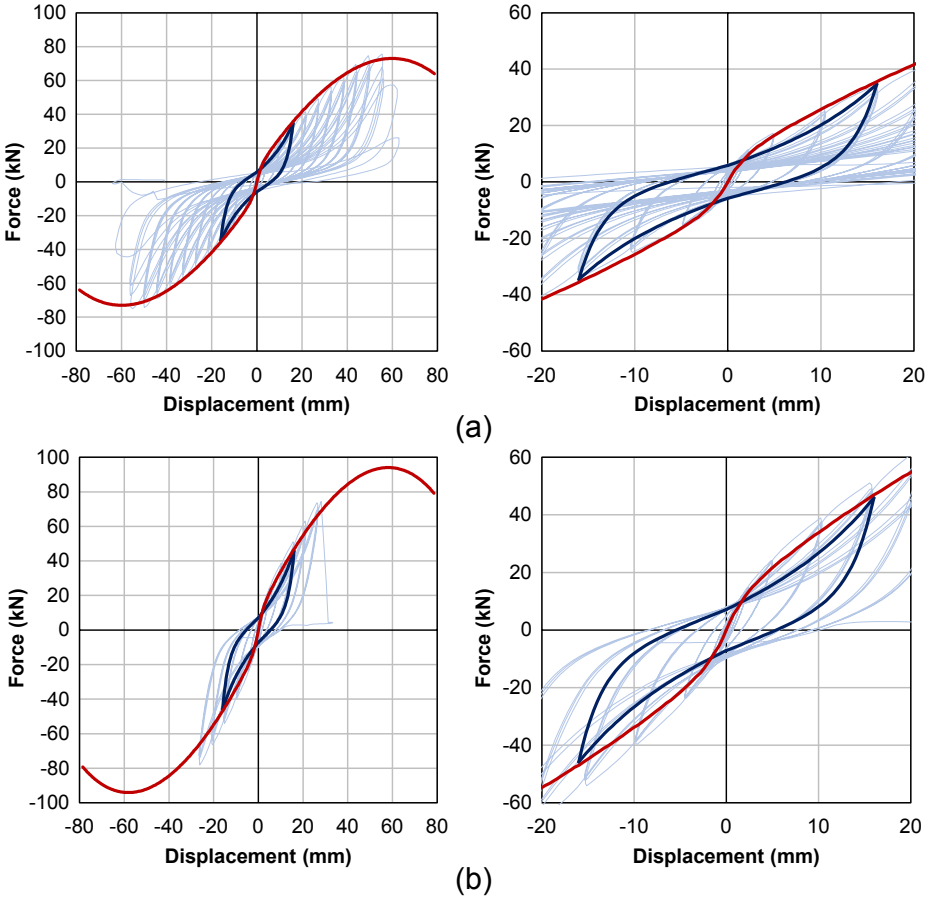

Fig. 10. Comparison between analytical backbone (red) and estimated pinching cycle (dark blue) with the experimental hysteretic response (light blue) for the floors tested parallel to the joists [14]: global (left) and initial (right) response of samples *DFpar-1 s* (a) and *DFpar-2 s* (b). (For interpretation of the references to colour in this figure legend, the reader is referred to the web version of this article.)

B. ($\delta_c/2$, intersection between bisector, and line joining $2/3\,F_0$ with the bisector at $\delta_c/2$);
C. (δ_c, $F_c(\delta_c)$);
D. Intersection between the line passing through $-2/3\,F_0$ parallel to the one individuating point B, and the branch with slope K_0;
E. (0, $-2/3F_0$).

The negative part of the pinching cycle (points B', C', D' of Fig. 9) is antisymmetric to the positive one, as defined for the equation of the backbone curve. The reference points can be directly adopted for implementation (for instance, when using *Pinching4* material in *OpenSees*; see Section 5).

For a more refined analytical evaluation of both pinching and damping properties of the diaphragms, the multilinear cycle is used in step 5 to construct four exponential branches smoothening the straight lines. The equations link these straight lines similarly to Foschi's formulation [18]. Considering, for more simplicity in deriving the expressions and aided by Fig. 9, the negative part of the pinching cycle ($\delta_{C'} \leq \delta \leq 0$), the equations are:

- Negative loading:

$$F_{nl} = F_{C'} + \left[\left(F_E - F_{C'} + \frac{F_E - F_{B'}}{\delta_E - \delta_{B'}}\delta_{C'}\right) + \frac{F_E - F_{B'}}{\delta_E - \delta_{B'}}(\delta - \delta_{C'})\right] \left[1 - \exp\left(-\frac{D_p \frac{F_{B'} - F_{C'}}{\delta_{B'} - \delta_{C'}}}{F_E - F_{C'} + \frac{F_E - F_{B'}}{\delta_E - \delta_{B'}}\delta_{C'}}(\delta - \delta_{C'})\right)\right] \quad (15)$$

where $D_p = 1 + (\delta_{C'}/\delta_{max})^3$ is a factor accounting for pinching stiffness degradation, dependent on the displacement δ_{max} at which the diaphragm's peak force is reached. This factor implies that the loading branch follows the bisector's slope (segment C'-B') for small displacements, but then its slope increases up to two times the bisector's one at δ_{max}. With this additional factor, it is therefore possible to account for stiffness degradation depending on the reached displacement.

- Negative unloading:

$$F_{nu} = F_{C'} + \left[\left(F_A - F_{C'} + \frac{F_A - F_{D'}}{\delta_A - \delta_{D'}}\delta_{C'}\right) + \frac{F_A - F_{D'}}{\delta_A - \delta_{D'}}(\delta - \delta_{C'})\right] \left[1 - \exp\left(-\frac{2\frac{F_{D'} - F_{C'}}{\delta_{D'} - \delta_{C'}}}{F_A - F_{C'} + \frac{F_A - F_{D'}}{\delta_A - \delta_{D'}}\delta_{C'}}(\delta - \delta_{C'})\right)\right] \quad (16)$$

Then, for the positive part of the pinching cycle ($0 \leq \delta \leq \delta_C$), the other two curves F_{pl} (positive loading) and F_{pu} (positive unloading) are antisymmetric to the aforementioned ones. Since the initial unloading stiffness of pinching cycles is usually quite high, this was taken as $2K_0$, as can be noticed in Eq. (16). Finally, each curve is asymptotic, thus in $\delta = 0$ continuity is not guaranteed. To adjust for this, the curves F_{pl} and F_{nu} are translated along the y-direction by the quantity $[F_{pl}(0)–F_{nu}(0)]/2$, to have a common $F(0)$ at $[F_{pl}(0)+F_{nu}(0)]/2$; the curves F_{pu} and F_{nl} are translated along the y-direction by the quantity $[F_{pu}(0)–F_{nl}(0)]/2$, to have a common $F(0)$ at $[F_{pu}(0)+F_{nl}(0)]/2$.

This completes the analytical derivation of the pinching cycle. The advantage of this geometrical procedure is that the pinching cycle can

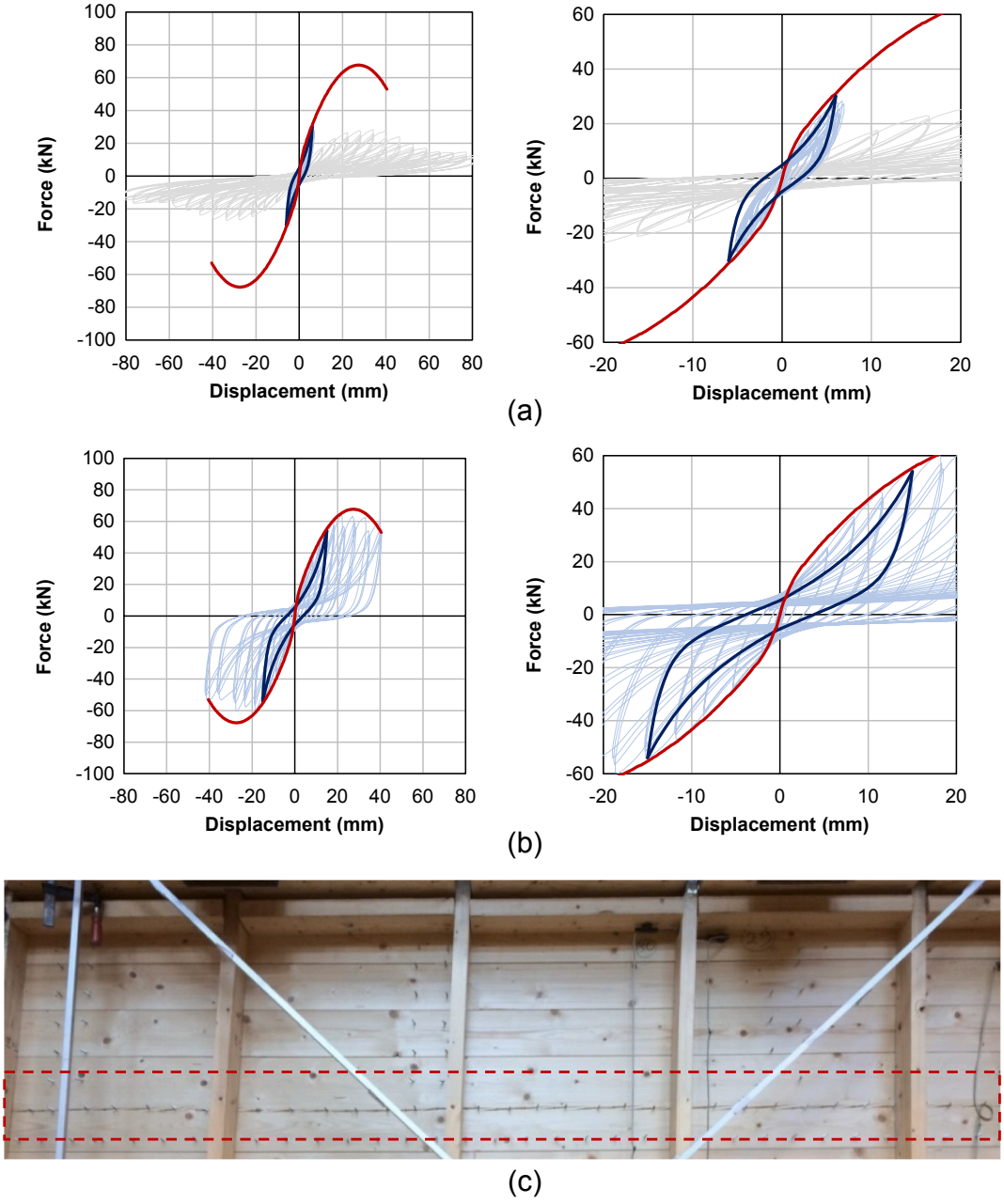

Fig. 11. Comparison between analytical backbone (red) and estimated pinching cycle (dark blue) with the experimental hysteretic response (light blue) for the floors tested perpendicular to the joists [14]: global (left) and initial (right) response of samples *DFper-3s* (a, with in grey the overall recorded cycle and light blue the sheathing's one) and *DFper-4s* (b); crack opening in a plank during softening phase of sample *DFper-4s* (c). (For interpretation of the references to colour in this figure legend, the reader is referred to the web version of this article.)

follow the nonlinear behaviour of the backbone curve, because of the progressive change of slope of the bisector (Fig. 9, step 6). This estimation of the pinching cycle proved to be reliable, as will be shown in Section 4.

4. Results of the application of the analytical model to the tested floors

The combination of the derived analytical curve and of the pinching cycle estimation enables the prediction of the tested floor's response, in order to assess the reliability of the developed model. Therefore, this section presents a comparison of the analytical backbone (always depicted in red) and an estimated representative pinching cycle (always shown in dark blue), with the experimental hysteretic cycles (light blue). The results are presented in Figs. 10–12: for each diaphragm, both the global behaviour and the initial response (up to 20 mm displacement) are shown. As can be noticed, the analytical model proves to well predict the in-plane behaviour of the diaphragms, also when variations are present with respect to the reference tests on plank-plywood panel joints.

For sample *DFpar-1s* (Fig. 10a), the initial stiffness and pinching response are fully captured by the model. Besides, the fact that panel interlocking is taken into account enables the correct prediction of both strength and displacement at failure of the specimen. The softening behaviour was not fully achieved during the test, because of premature failure of the screws and nails enabling the shear transfer on the floor side. By adopting more fasteners, the failure would have been distributed only among the panels screws, leading to the behaviour described

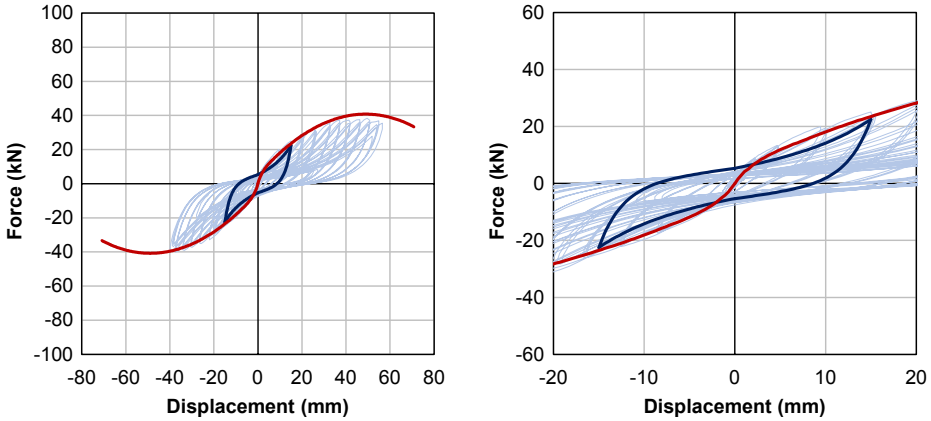

Fig. 12. Comparison between analytical backbone (red) and estimated pinching cycle (dark blue) with the experimental hysteretic response (light blue) for the roof pitch [14]: global (left) and initial (right) response of sample *DFpar-5s*. (For interpretation of the references to colour in this figure legend, the reader is referred to the web version of this article.)

by the model.

In sample *DFpar-2s* (Fig. 10b), both initial stiffness and pinching behaviour are well predicted by the developed model, with a slight load underestimation, especially for the negative backbone. Nevertheless, the global response appears to be properly captured, but in this case the diaphragm was not tested until capacity, because of the failure of the bottom glue layer anchoring it to the laboratory floor [14].

Sample *DFper-3s* was characterized by the failure of the nails connecting joists and planks on the top part of the floor, leading to a decrease in stiffness and a softening phase [14]: this failure caused the joists to move independently from the sheathing, which underwent a lower deflection. The global response of the specimen is depicted in grey in Fig. 11a and seems not to be represented by the model. However, this overall response recorded by the reference sensor included the independent movement of the joists: instead, when considering the sensor recording only the sheathing's behaviour (planks and plywood system, light blue), the latter is again correctly predicted in terms of initial stiffness and pinching behaviour.

This is even more evident in sample *DFper-4s*, identical to *DFper-3s*, but in which timber blocks were placed to prevent the aforementioned independent movement of the joists. In this case, both initial and the global behaviour of the floor are predicted by the model, including peak force and displacement at which this takes place. During the test, after beginning the softening phase, besides yielding of the screws, also cracking of the plywood panels and planks along one row of fasteners occurred (Fig. 11c): this led to a free sliding of the sheathing for larger drifts, thus Fig. 11b shows the floor's hysteretic cycles up to the displacement at which the crack occurred.

Finally, the model proved to be effective also for the roof pitch (sample *DFpar-5s*), again for both initial response and global behaviour, including failure of the sample. The pinching response is properly captured as well.

The graphical comparison of Figs. 10–12 is completed by Table 6, in which the values of floor's initial stiffness, peak force and its corresponding displacement are reported, from both experimental tests and analytical calculations; the observed failure modes are also summarized. The bottom glue layer failure in sample *DFpar-2s* would not occur in practice, because it would not be part of the retrofitting: it was only needed to complete the bottom clamping of the floors for the tests [14]. Instead, boundary conditions have to be appropriately designed, to achieve a more gradual and global failure of the retrofitted diaphragms, as obtained for instance with sample *DFpar-5s*. Furthermore, in the context of the global seismic response of existing buildings, out-of-plane walls cannot be subjected to excessive deflections. Thus, an accurate characterization of the floors behaviour until moderate drift limits is of importance, and the proposed analytical model proved to be suitable for this purpose, as can also be noticed by the good estimation of the diaphragms initial stiffness K_0 in Table 6.

Table 6
Comparison between initial stiffness K_0, peak force F_{max} and corresponding displacement d_{max} obtained from test results and calculated with the analytical model. The cause of failure observed during the tests is also reported for each sample.

Sample	Test results				Results from analytical model		
	Cause of failure [11]	K_0 (kN/mm)	F_{max} (kN)	d_{max} (mm)	K_0 (kN/mm)	F_{max} (kN)	d_{max} (mm)
DFpar-1s	Top row of screws, global plasticization	5.4	75.6	55.5	5.2	73.0	59.9
DFpar-2s	Bottom glue layer	6.3	Not reached		6.6	94.1	58.1
DFper-3s	Joists nails	10.8	Not reached		11.2	67.7	27.3
DFper-4s	Yielding of screws, splitting in a plank	11.8	64.1	22.0	11.2	67.7	27.3
DRpar-5s	Bottom bolts, global plasticization	3.5	38.4	49.6	3.8	40.8	48.8

Besides, if the screws are all placed at the same spacing, a quick prediction of the diaphragms strength can also be performed by considering the resistance of the fasteners in the top horizontal line, according to the static scheme already shown in Fig. 7. Table 7 reports the results from these calculations, in comparison to the experimental outcomes. Again, as can be noticed, comparable values are found. The strength of samples *DFpar-1s* and *DFpar-2s* is slightly underestimated with this method, because the drift-dependent influence of panels

Table 7
Comparison between the diaphragms strength evaluated from the resistance of the fasteners in the top horizontal line, and the experimental strength for the five tested diaphragms.

Sample	Strength of one screw (kN)	Number of screws in the top horizontal line (kN)	Diaphragm's strength from screws in the top horizontal line (kN)	Experimental diaphragm's strength (kN)
DFpar-1s	1.6	42	67.2	75.6
DFpar-2s	2.0	44	88.0	Not reached, expected 94.1
DFper-3s	1.8	38	68.4	Not reached, expected 67.7
DFper-4s	1.8	38	68.4	64.1
DRpar-5s	1.6	32	51.2	38.4

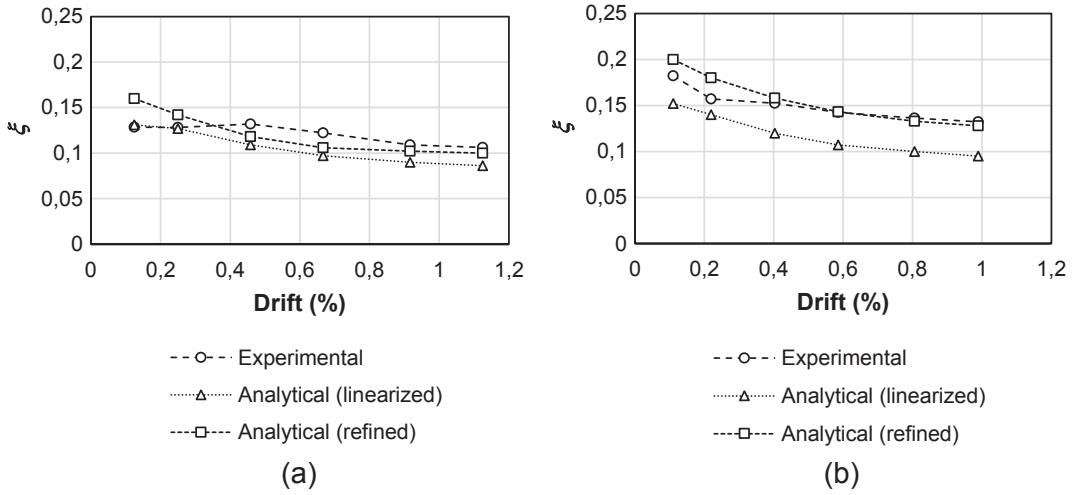

Fig. 13. Example of comparison, for (a) a floor (*DFpar-2s*) and (b) a roof sample (*DRpar-5s*), between the analytically predicted equivalent damping ratio (adopting both the linearized and the refined pinching cycle) and the one calculated in [27] from the tests presented in [11].

interlocking (Eqs. (11) and (12)) is not taken into account. For specimen *DRpar-5s*, a higher strength value is found, because in that case the screws in the vertical lines are governing: due to the presence of purlins, their spacing is increased compared to the one of the top horizontal line of screws; therefore, the latter group of fasteners provides more resistance.

With this procedure, it is possible to guarantee that sufficient shear transfer is provided by the diaphragm, according to the expected horizontal loads. The proposed analytical model completes the characterization of the floors in-plane response with the calculation of the deflection, and the evaluation of nonlinearities and energy dissipation.

In terms of energy dissipation, pinching cycles are well predicted for all samples, and provide equivalent damping ratio (ξ) values close to experimental ones (Fig. 13), as determined in [27] by means of the energy loss per cycle method [28]. It can be noticed that the use of the simplified multilinear pinching cycle tends to underestimate the dissipative contribution of the floor, while the refined one provides more reliable results, especially for drifts larger than 0.4%.

5. Example of implementation of the model and recommendations

The developed analytical procedure can be used as input for numerical models or further calculations, and in particular the following applications can be of interest:

- When performing simplified analyses on the seismic response of retrofitted existing buildings, it is important to correctly estimate the in-plane stiffness of the strengthened timber diaphragms. The proposed model can provide a reliable value for it that depends on the reached drift, instead of using a generalized equivalent shear stiffness.
- If advanced analyses are conducted, then the full nonlinear and cyclic in-plane response of the floors is of interest, and this is well predicted by the analytical model. Therefore, a proper implementation can be performed, depending on the purpose of the analyses.

With reference to the second point, it is important to distinguish between applications in which the aim is to assess the overall response of the diaphragms (up to failure), and analyses for which the target is the global behaviour of a building. This distinction will be presented taking into account the implementation procedure adopted for the *Pinching4* material type [25] in *OpenSees* [26], which proves to be quite accurate for these applications. The pinching cycle is identified as a succession of linear branches, as is already considered for the analytical model, but the backbone curve has to be constructed with four points (Fig. 14). Therefore, from the analytical curve a proper implementation of the backbone one has to be carried out.

In the first case, when the total deflection range of the floor is of interest (Fig. 14a), the backbone curve can be constructed considering

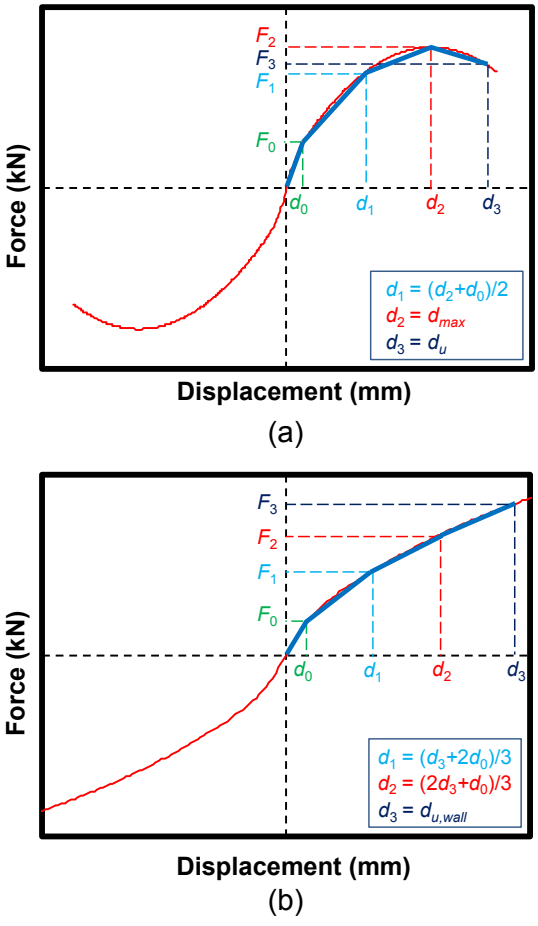

Fig. 14. Implementation procedure of the analytical model based on *OpenSees Pinching4* material [25] when the aim is to model the global response of the floors (a) or their nonlinear behaviour in a whole building (b).

the whole analytical curve, as can be noticed. The ultimate displacement d_3 corresponds to the diaphragm's failure ($F_3 = 0.8F_{max}$). In order to obtain a reliable result, since *OpenSees* creates by default a drift-dependent evolution in terms of stiffness and enclosed area for pinching, it is advised to estimate the input cycle at d_1. In this way, it is possible to avoid an overestimation of the floor's energy dissipation due to the choice of a reference cycle too close to the beginning of the load–displacement history.

When, instead, the target is the seismic assessment of a whole building, it is important to well characterize the floor until the expected drift, beyond which, for instance, the out-of-plane failure of the wall may occur. In this case, the response of the diaphragms has to be modelled thoroughly in terms of stiffness and energy dissipation, but only for a limited initial part of the backbone curve (Fig. 14b), as derived according to the storey seismic shear when designing the retrofitted floor and its connections to the walls. Therefore, after having determined the maximum out-of-plane drift for the wall ($d_{u,wall}$), the remaining part of the backbone can be constructed. As a final step, for the same reason as in the previous case, it is advised to estimate the input pinching cycle at d_2.

The two aforementioned procedures were both applied to sample *DFpar-1 s*, as a representative example. The modelling strategy is shown, together with the results, in Fig. 15. The numerical model consisted of a grid of infinitely stiff truss elements, in which diagonal nonlinear springs were inserted, with the *Pinching4* material implemented in them, according to the indications given for either the global or the initial response of the floor. Starting from the backbone curve of the whole diaphragm, it is possible to define the constitutive law for the single spring according to geometrical considerations. The displacement δ of the spring is given by:

$$\delta = \frac{u}{m}\cos\alpha \tag{17}$$

where α is the angle between the spring and the loading direction (Fig. 15a) and m the number of macro-elements rows parallel to the applied load (in this case, $m = 2$). The shear force F is then subdivided among the s springs in a macro-elements row, and transformed into an axial force N on a single one:

$$N = \frac{F}{s\cos\alpha} \tag{18}$$

Cyclic displacement-based analyses were performed, similarly to the experimental tests: the results confirm that the analytical model can be reliably adopted as an input for the numerical one, and the two proposed procedures can be suitably applied to determine the global or initial diaphragm's behaviour. In the proposed example, since the analytical model slightly underestimates the peak force, this is reflected in the numerical model as well. However, the overall response appears still to be well captured (Fig. 15b). An even better result is achieved for the

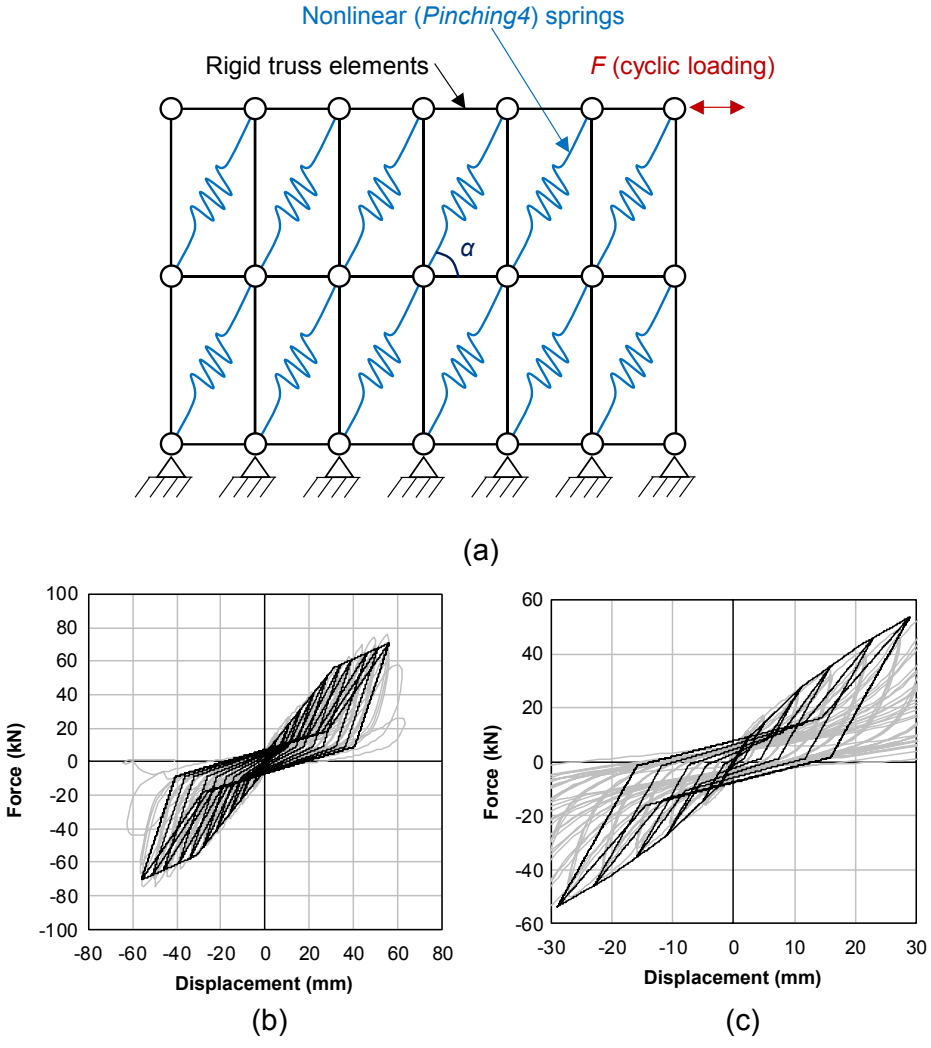

Fig. 15. Numerical model for the diaphragm representation (a); results of the numerical analysis when implementing the analytical model to assess the global (b) and initial (c) response of the diaphragms. The experimental cycle (grey) refers to sample *DFpar-1s*, the numerical cycle is depicted in black.

initial behaviour of the floor, due to the accuracy of the model in predicting the beginning of the load–displacement curve (Fig. 15c).

6. Summary and conclusions

In this work, an analytical model was presented, predicting the in-plane behaviour and the dissipative properties of timber diaphragms strengthened with plywood panels. The proposed formulation starts from the definition of a load-slip equation for the single screw, fastening plywood panel and plank. This expression was derived from both performed tests, and also through equations from standards or literature: this allowed to generalize the model and to account for variations with respect to the performed reference tests as well. In this way, even when tests are not available, it is possible to derive this model following the provided guidelines.

The proposed equation enables an accurate prediction of the load-slip response of a single screw: starting from this analytical curve, it is possible to derive the whole diaphragm's in-plane backbone curve, and the pinching cycles at chosen displacements. By putting together the backbone curve and the pinching cycles, reliable input values for numerical analyses can be retrieved, as well as an accurate estimation of the evolution of the floors in-plane stiffness with its drift. Further research is ongoing related to the implementation of the analytical model via user-supplied subroutines in other software besides *OpenSees*.

In conclusion, with this model it is possible to avoid the use of general values of shear stiffness to characterize the in-plane behaviour of these retrofitted timber diaphragms, because with the proposed formulation the expected load is known for each displacement level. Therefore, an equivalent secant stiffness can always be calculated to precisely describe the response of the floors. Moreover, the model can be used to efficiently design strengthening interventions with plywood panels for timber floors in existing buildings, with a more reliable assessment of the impact of the retrofitted diaphragms on the global response of the structures.

CRediT authorship contribution statement

Michele Mirra: Conceptualization, Methodology, Software, Validation, Formal analysis, Investigation, Writing - original draft, Visualization. **Geert Ravenshorst:** Conceptualization, Methodology, Supervision, Writing - review & editing, Project administration, Funding acquisition. **Peter Vries:** Conceptualization, Methodology, Writing - review & editing. **Jan-Willem Kuilen:** Writing - review & editing, Project administration, Funding acquisition.

Declaration of Competing Interest

The authors declare that they have no known competing financial interests or personal relationships that could have appeared to influence the work reported in this paper.

Acknowledgements

The authors thankfully acknowledge NAM (*Nederlandse Aardolie Matschappij*) for the financial support given to this study (grant no. C31B67).

References

[1] Piazza M, Baldessari C, Tomasi R. The Role of In-Plane Floor Stiffness in the Seismic Behaviour of Traditional Buildings. 14th World Conference on Earthquake Engineering. 2008.
[2] Baldessari C. In-plane behaviour of differently refurbished timber floors. Ph.D. Thesis, University of Trento; 2010.
[3] Modena C, Valluzzi MR, Garbin E, da Porto F. A strengthening technique for timber floors using traditional materials. Proceedings of the Fourth International Conference on Structural Analysis of Historical Constructions SAHC 04, Padua, Italy, 10–13 November 2004, pp. 911–921; 2004.
[4] Valluzzi MR, Garbin E, Dalla Benetta M, Modena C. In-plane strengthening of timber floors for the seismic improvement of masonry buildings. In: 11th World Conference on Timber Engineering, Riva del Garda; 2010.
[5] Valluzzi MR, Garbin E, Dalla Benetta M, Modena C. Experimental assessment and modelling of in-plane behaviour of timber floors. D. D'Ayala and E. Fodde (Eds.), Proceedings of the VI International Conference on Structural Analysis of Historic Construction, SAHC 08, 2–4 July 2008, Bath, UK; 2008. p. 755–762.
[6] Gattesco N, Macorini L. High reversibility technique for in-plane stiffening of wooden floors. In: D'Ayala D, Fodde E (Eds.), Proceedings of the VI international conference on structural analysis of historic construction, SAHC 08, 2–4 July 2008, Bath, UK, 2008, pp. 1035–1042.
[7] Corradi M, Speranzini E, Borri A, Vignoli A. In-plane shear reinforcement of wood beam floors with FRP. Compos B 2006;37:310–9.
[8] Branco JM, Kekeliak M, Lourenço PB. In-plane stiffness of timber floors strengthened with CLT. Eur J Wood Products 2015;73:313–23.
[9] Gubana A, Melotto M. Experimental tests on wood-based in-plane strengthening solutions for the seismic retrofit of traditional timber floors. Constr Build Mater 2018;191:290–9.
[10] Rizzi E, Capovilla M, Piazza M, Giongo I. In-plane behaviour of timber diaphragms retrofitted with CLT panels. Chapter in book: R. Aguilar et al. (Eds.): Structural Analysis of Historical Constructions, RILEM Bookseries 18, (2019), pp. 1613-1622.
[11] Peralta DF, Bracci MJ, Hueste MBD. Seismic behavior of wood diaphragms in pre-1950s unreinforced masonry buildings. J Struct Eng 2004;130:2040–50.
[12] Brignola A, Pampanin S, Podestà S. Experimental evaluation of the in-plane stiffness of timber diaphragms. Earthquake Spectra 2012;28(4):1–23.
[13] Wilson A, Quenneville PJH, Ingham JM. In-plane orthotropic behavior of timber floor diaphragms in unreinforced masonry buildings. J Struct Eng 2014;140.
[14] Mirra M, Ravenshorst G, van de Kuilen J-W. Experimental and analytical evaluation of the in-plane behaviour of as-built and strengthened traditional wooden floors. Eng Struct 2020;211. https://doi.org/10.1016/j.engstruct.2020.110432.
[15] Rizzi E, Giongo I, Ingham J, Dizhur D. Testing and modeling in-plane behavior of retrofitted timber diaphragms. J Struct Eng 2020;146:2.
[16] Gubana A. State-of-the-Art Report on high reversible timber to timber strengthening interventions on wooden floors. Constr Build Mater 2015;97:25–33.
[17] ISO 16670:2003. Timber structures — Joints made with mechanical fasteners — Quasi-static reversed-cyclic test method. ISO (International Organization for Standardization).
[18] Foschi RO. Load-slip characteristics of nails. Wood Sci 1974;17:69–77.
[19] EN 12512:2001. Timber Structures – Test Methods – Cyclic Testing of Joints Made with Mechanical Fasteners. CEN (European Committee for Standardization).
[20] Dubas P, Gehri E, Steurer T. Einführung in die Norm SIA 164 (1981) – Holzbau. Publication No. 81-1, Baustatik und Stahlbau, ETH Zürich, Switzerland; 1981.
[21] EN 1995-1-1:2004+A2:2014. Eurocode 5: Design of timber structures - Part 1-1: General - Common rules and rules for buildings. CEN (European Committee for Standardization).
[22] DIN 1052:2008. Entwurf, Berechnung und Bemessung von Holzbauwerken - Allgemeine Bemessungsregeln und Bemessungsregeln für den Hochbau. Deutsches Institut für Normung e.V., Berlin, Germany.
[23] EN 409:2009. Timber structures - Test methods - Determination of the yield moment of dowel type fasteners. CEN (European Committee for Standardization).
[24] Johansen KW. Theory of timber connections. Publ. 9 Bern. International Association of Bridge and Structural Engineering; 1949.
[25] Mazzoni S, McKenna F, Scott MH, Fenves GL. OpenSees Command Language Manual. University of California, Berkeley, 2006. Link: http://opensees.berkeley.edu/manuals/usermanual.
[26] McKenna F, Fenves GL, Scott MH. Open system for earthquake engineering simulation. University of California, Berkeley CA. Link: http://opensees.berkeley.edu.
[27] Mirra M, Ravenshorst G, van de Kuilen J-W. Dissipative properties of timber diaphragms strengthened with plywood panels. In: Proceedings of the 16th World Conference on Timber Engineering, Santiago, Chile, 9-12 August 2021. (submitted).
[28] Clough RW, Penzien J. Dynamics of structures. McGraw-Hill New York 1993.